

Dear Author,

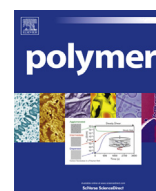
Please, note that changes made to the HTML content will be added to the article before publication, but are not reflected in this PDF.

Note also that this file should not be used for submitting corrections.



Contents lists available at ScienceDirect

Polymer

journal homepage: [www.elsevier.com/locate/polymer](http://www.elsevier.com/locate/polymer)

# Hepatocyte-targeted fluorescent nanoparticles based on a polyaspartamide for potential theranostic applications

Emanuela Fabiola Craparo<sup>a</sup>, Mariano Licciardi<sup>a</sup>, Alice Conigliaro<sup>b,c</sup>,  
Fabio Salvatore Palumbo<sup>a</sup>, Gaetano Giammona<sup>a</sup>, Riccardo Alessandro<sup>b</sup>,  
Giacomo De Leo<sup>b</sup>, Gennara Cavallaro<sup>a,\*</sup>

<sup>a</sup> Dipartimento di Scienze e Tecnologie Biologiche Chimiche e Farmaceutiche (STEBICEF), Università di Palermo, Palermo, Italy

<sup>b</sup> Dipartimento di Biopatologia e Biotecnologie Mediche e Forensi (Di.Bi.Me.F.), Università di Palermo, Palermo, Italy

<sup>c</sup> Dipartimento di Biotecnologie Cellulari ed Ematologia, Sapienza Università di Roma, Rome, Italy

## ARTICLE INFO

### Article history:

Received 15 April 2015

Received in revised form

4 June 2015

Accepted 9 June 2015

Available online xxx

### Keywords:

Active targeting

$\alpha,\beta$ -Poly-(N-2-hydroxyethyl)-DL-aspartamide (PHEA)

Fluorescence imaging

Graft copolymers

Nanoparticles

## ABSTRACT

Here, the synthesis of a galactosylated amphiphilic copolymer bearing rhodamine (RhB) moieties and its use for the preparation of polymeric fluorescent nanoparticles for potential applications in therapy and diagnosis are described.

To do this, firstly, a fluorescent derivative of  $\alpha,\beta$ -poly(N-2-hydroxyethyl)-DL-aspartamide (PHEA) was synthesized by chemical reaction with RhB, and with polylactic acid (PLA), to obtain PHEA-RhB-PLA. Then, the derivatization of PHEA-RhB-PLA with GAL-PEG-NH<sub>2</sub> allows obtaining PHEA-RhB-PLA-PEG-GAL copolymer, with derivatization degrees in -PLA and -PEG-GAL equal to 1.9 mol% and 4.5 mol%, respectively. Starting from this copolymer, liver-targeted fluorescent nanoparticles were prepared by high pressure homogenization–solvent evaporation method, and showed nanoscaled size, slightly negative zeta potential and spherical shape. Chemical and enzymatic stability of fluorescent dye covalently linked to the copolymer backbone by ester linkage was demonstrated until 4 days of incubation. Finally, thanks to the covalently-linked fluorescent RhB, it was demonstrated that these galactosylated nanoparticles interact with HepG2 cells that are positive for the asialoglycoprotein receptor (ASGPR), while these do not interact with HeLa cells that are negative for the same receptor, demonstrating the contributor of ASGPR to the internalization process.

© 2015 Published by Elsevier Ltd.

## 1. Introduction

In the field of nanomedicine, the use of polymeric nanoparticles bearing a fluorescent probe for imaging is a promising application to evaluate intracellular trafficking and/or events, and body distribution of therapeutic systems, in a non-invasive way [1]. Moreover, the potential of these systems to enable the detection of many processes inside the cells, could allow the understanding of disfunctionalities and the subsequent occurrence of diseases. Some of these fluorescent polymer-based systems are currently proposed for simultaneous applications combining both therapy and diagnosis [2,3].

To realize fluorescent polymer-based nanoparticles, the polymeric materials used as the matrix should offer excellent

biocompatibility, multiple functional groups for further conjugation with dyes, drugs, and/or targeting ligands, and the ability to form stable particles that persist over a long time also in biological environments. Moreover, by varying the polymer, the preparation method, and the kind of surface functionalization, it is possible to precisely engineer these particles to a specific application.

Complementary to the passive targeting to an organ or a tissue, which is mainly obtained with nanoparticles with high circulation time depending on their size, shape, surface charge and chemistry, active targeting with ligands can also be exploited to reach cell specificity [1]. A targeting moiety can be conjugated to the fluorescent particle to improve the localization and binding of the dye in the area to image, and to modify its pharmacokinetics. The targeting moiety can be for instance an antibody, protein or peptide, an oligonucleotide, a saccharide, or any other molecular template known for its specific affinity for a cellular compartment, cellular receptor, biological fluid or tissue [4].

\* Corresponding author. Dipartimento di Scienze e Tecnologie Biologiche Chimiche e Farmaceutiche (STEBICEF), Università di Palermo, via Archirafi 32, 90123 Palermo, Italy.

E-mail address: [gennara.cavallaro@unipa.it](mailto:gennara.cavallaro@unipa.it) (G. Cavallaro).

Galactosylation is a well-established strategy to obtain a hepatocyte active targeting because targeting via galactosylated carriers exploits highly specific interactions of galactose ligands with asialoglycoprotein receptor (ASGPR) that is specifically and abundantly found on hepatocytes [5,6].

In this paper, the realization of fluorescent polymeric nanoparticles targeted to hepatocytes by following easily scaling up processes and by using starting materials with suitable structural and functional properties, is reported. In particular, the synthesis of a fluorescent amphiphilic polyaspartamide-based copolymer starting from  $\alpha,\beta$ -poly(*N*-2-hydroxyethyl)-DL-aspartamide (PHEA) is reported. PHEA is a biocompatible, synthetic protein-like polymer, already used for obtaining polymeric carriers with potential application in controlled and targeted drug delivery [6–10]. PHEA was functionalised with rhodamine B, with acid terminated PLA and with a galactosylated PEG derivative in order to obtain PHEA-RhB-PLA-PEG-GAL graft copolymer. The latter was used for the preparation of liver-targeted fluorescent polymeric nanoparticles by using the high pressure homogenization-solvent evaporation technique [11], without the use of surfactants or stabilizing agents. Obtained nanoparticles showed nanometric size, spherical shape, low surface charge, and were stable after dispersion in physiological-mimicking condition until 24 h. Moreover, stability of linkage of RhB on these polymeric nanoparticles until 4 days was also demonstrated. Preliminary in vitro studies demonstrated the absence of cell toxicity, and the contributor of ASGPR to the internalization process of galactosylated nanoparticles in HepG2 cells.

## 2. Experimental

### 2.1. Materials

Rhodamine B (RhB), anhydrous *N,N'*-dimethylformamide (*a*-DMF),  $\alpha$ -lactose, D,L-poly(lactic acid) (PLA acid terminated,  $M_w = 10$ –18 kDa), sodium cyanoborohydride, 1,1'-carbonyldiimidazole (CDI), *N,N'*-disuccinimidyl carbonate (DSC), anthrone, anhydrous dimethylacetamide (*a*-DMA), poly(ethylene oxide) standards, esterase from porcine liver or lipase from porcine pancreas type II were purchased from Sigma–Aldrich (Italy). Diethylamine (DEA), triethylamine (TEA), O-(2-aminoethyl)-O'-methyl poly(ethylene glycol) 2000 (PEG<sub>2000</sub>) ( $\leq 0.4$  mmol NH<sub>2</sub>/g), poly(ethylene glycol)bis(amine) 2000 (H<sub>2</sub>N-PEG-NH<sub>2</sub>), ethyl ether, dichloromethane were obtained from Fluka (Italy). All reagents were of analytic grade, unless otherwise stated.

$\alpha,\beta$ -Poly(*N*-2-hydroxyethyl)-D,L-aspartamide (PHEA) was prepared by aminolysis of polysuccinimide (PSI) with ethanolamine in DMF solution [12]. Spectroscopic data were in agreement with the attributed structure [12]. Weight average molecular weight ( $\bar{M}_w$ ) of PHEA was 38.7 kDa ( $\bar{M}_w/\bar{M}_n = 1.62$ ), determined by SEC analysis.

The SEC system (Waters, Milford, MA) was equipped with a pump system, two Phenogel columns from Phenomenex (5  $\mu$ m particle size,  $10^3$  Å and  $10^4$  Å of pores size), and a 410 differential refractometer (DRI) as concentration detector. Analyses were performed with 0.01 M LiBr DMF solution as eluent with a flow of 0.8 ml/min and poly(ethylene oxide) standards (range 145–1.5 kDa) to obtain the calibration curve. The column temperature was set at 50 °C ( $\pm 0.1$  °C).

### 2.2. Synthesis of PHEA-RhB copolymer

Derivatization of PHEA with RhB to obtain the PHEA-RhB copolymer was carried out by using CDI as coupling agent to activate the RhB carboxyl groups. A calculated amount of CDI dissolved in *a*-DMF (26.0 mg/ml) under argon atmosphere, was added drop-

wise to a RhB solution in *a*-DMF (8.7 mg/ml), according to  $R_1 = 1.25$  being:

$$R_1 = \frac{\text{moles of CDI}}{\text{moles of RhB}} \quad (1)$$

The clear solution was stirred at 40 °C for 4 h under argon atmosphere. Simultaneously, 33.3 mg/ml of PHEA were dissolved in *a*-DMF at 40 °C under argon atmosphere and then DEA, as catalyst, was added. The amounts of PHEA and DEA were calculated according to  $R_2 = 0.01$  and  $R_3 = 5$ , being:

$$R_2 = \frac{\text{moles of RhB}}{\text{moles of hydroxyl – carrying PHEA repeating units}} \quad (2)$$

$$R_3 = \frac{\text{moles of DEA}}{\text{moles of RhB}} \quad (3)$$

After activation time, the resulting polymeric solution was added drop-wise and slowly to CDI-activated RhB (aRhB) solution. The reaction mixture was left under argon atmosphere and continuous stirring at 40 °C for 48 h, then was precipitated in diethyl ether and the suspension was centrifuged at 4 °C for 15 min, at 9800 rpm by using a Centra MP4R IEC centrifuge, equipped with a 854 rotor and temperature control. The obtained solid product was recovered, washed four times with ethanol, separating the washing mixture by centrifugation at 4 °C for 15 min, at 9800 rpm. Then, the product, dried under vacuum, was obtained with a yield of 85 wt% based on the starting PHEA weight.

### 2.3. Characterization of PHEA-RhB copolymer

PHEA-RhB derivative was characterized by <sup>1</sup>H NMR and SEC analyses.

<sup>1</sup>H NMR spectra were obtained by a Bruker Avance II-300 spectrometer, working at 300 MHz. <sup>1</sup>H NMR (300 MHz, D<sub>2</sub>O, 25 °C, TMS):  $\delta$  1.15 (m, 12H<sub>RhB</sub> CH<sub>3</sub>–CH<sub>2</sub>–);  $\delta$  2.71 (m, 2H<sub>PHEA</sub> –CO–CH–CH<sub>2</sub>–CO–NH–);  $\delta$  3.29 (t, 2H<sub>PHEA</sub> –NH–CH<sub>2</sub>–CH<sub>2</sub>–O–);  $\delta$  3.58 (t, 2H<sub>PHEA</sub> –NH–CH<sub>2</sub>–CH<sub>2</sub>–O–);  $\delta$  4.65 (m, 1H<sub>PHEA</sub> –NH–CH(CO)CH<sub>2</sub>–);  $\delta$  8.00–8.50 (m, 10H<sub>RhB</sub> H–Ar).  $\bar{M}_w$  of PHEA-RhB graft copolymer, determined by SEC analysis, was found to be 35.0 kDa ( $\bar{M}_w/\bar{M}_n = 1.41$ ).

### 2.4. Evaluation of molar extinction coefficient ( $\epsilon$ ) of PHEA-RhB

$\epsilon$  of RhB and PHEA-RhB were evaluated in bidistilled water, in concentration ranging between  $10^{-7}$ – $10^{-4}$  M, by recording UV spectra with a RF-5301PC spectrofluorometer (Shimadzu, Italy). The absorption at maxima wavelength was measured and the  $\epsilon$  was calculated from the curve obtained by plotting absorbance versus sample solution concentrations. Each experiment was repeated in triplicate. For RhB, the maxima wavelength was 554 nm ( $y = 117,044x$ ,  $R^2 = 0.9996$ ), while for PHEA-RhB was 561 nm ( $y = 53,200x$ ,  $R^2 = 0.99$ ).

### 2.5. Synthesis of PHEA-RhB-PLA graft copolymer

Derivatization of PHEA-RhB with acid terminated PLA to obtain the PHEA-RhB-PLA graft copolymer was carried out by using CDI as coupling agent. In particular, a calculated amount of CDI dissolved in *a*-DMF (123 mg/ml) under argon atmosphere, was added drop-wise to acid terminated PLA solution in *a*-DMF (175 mg/ml), according to  $R_4 = 2$  being:

$$R_4 = \frac{\text{moles of CDI}}{\text{moles of PLA}} \quad (4)$$

The clear solution was stirred at 40 °C for an activation time of 4 h under argon atmosphere. Simultaneously, 84 mg/ml of PHEA-RhB were dissolved in *a*-DMF at 40 °C under argon atmosphere and then DEA, as catalyst, were added. The amounts of acid terminated PLA and DEA were calculated according to  $R_5 = 0.06$  and  $R_6 = 8.5$ , being:

$$R_5 = \frac{\text{moles of PLA}}{\text{moles of hydroxyl – carrying PHEA – RhB repeating units}} \quad (5)$$

$$R_6 = \frac{\text{moles of DEA}}{\text{moles of PLA}} \quad (6)$$

After activation time, the resulting PHEA-RhB solution was added drop-wise and slowly to CDI-activated PLA (aPLA) solution. The reaction mixture was left under argon atmosphere and continuous stirring at 40 °C for 70 h, and then precipitated in diethyl ether:dichloromethane mixture (15:1 vol/vol). The obtained suspension was centrifuged at 4 °C for 15 min, at 9800 rpm, and the obtained solid product was recovered, washed four times with the same mixture, separating the washing mixture by centrifugation. Then, the solid product, dried under vacuum, was obtained with a yield of 280 wt% based on the starting PHEA-RhB weight.

## 2.6. Characterization of PHEA-RhB-PLA graft copolymer

PHEA-RhB-PLA derivative was characterized by  $^1\text{H}$  NMR and SEC analyses.

$^1\text{H}$  NMR (300 MHz, DMF- $d_7$ , 25 °C, TMS):  $\delta$  1.15 (m,  $12\text{H}_{\text{RhB}} \text{CH}_3\text{—CH}_2\text{—}$ );  $\delta$  1.3 and  $\delta$  1.7 (2d,  $582 \text{H}_{\text{PLA}} \text{—O—CO—CH(CH}_3\text{)—O—}$ );  $\delta$  2.8 (m,  $2\text{H}_{\text{PHEA}} \text{—CO—CH—CH}_2\text{—CO—NH—}$ );  $\delta$  3.3 (t,  $2\text{H}_{\text{PHEA}} \text{—NH—CH}_2\text{—CH}_2\text{—O—}$ );  $\delta$  3.59 (t,  $2\text{H}_{\text{PHEA}} \text{—NH—CH}_2\text{—CH}_2\text{—O—}$ );  $\delta$  4.2–4.5 and  $\delta$  5.1–5.5 (m,  $194 \text{H}_{\text{PLA}} \text{—O—CO—CH(CH}_3\text{)—}$ ), and  $\delta$  4.8 (m,  $1\text{H}_{\text{PHEA}} \text{—NH—CH(CO)CH}_2\text{—}$ );  $\delta$  7.0–8.0 (m,  $10\text{H}_{\text{RhB}} \text{H—Ar}$ ).  $\bar{M}_w$  of PHEA-RhB-PLA graft copolymer, determined by SEC analysis, was found to be 86.9 kDa ( $\bar{M}_w/\bar{M}_n = 1.45$ ).

## 2.7. Conjugation of lactose onto poly(ethylene glycol) bis(amine) ( $\text{H}_2\text{N-PEG-NH}_2$ )

The O-(2-aminoethyl)-O'-galactosyl polyethylene glycol ( $\text{H}_2\text{N-PEG-GAL}$ ) derivative was synthesized by a reductive amination reaction [13]. Briefly,  $\text{H}_2\text{N-PEG-NH}_2$  (50 mg/ml) was dissolved in borate buffer at pH 9, and solutions of lactose (171.2 mg/ml) and

$$R_7 = \frac{\text{moles of DSC}}{\text{moles of hydroxyl – carrying PHEA – RhB – PLA repeating units}} \quad (10)$$

sodium cyanoborohydride (31.4 mg/ml) were added, according to  $X = 2.5$ , where:

$$X = \frac{\text{moles of lactose}}{\text{moles of free – NH}_2 \text{ on H}_2\text{N – PEG – NH}_2} \quad (7)$$

and  $Y = 1$ , where

$$R_9 = \frac{\text{moles of – NH}_2 \text{ on H}_2\text{N – PEG – GAL}}{\text{moles of hydroxyl – carrying PHEA – RhB – PLA repeating units}} \quad (12)$$

$$Y = \frac{\text{moles of lactose}}{\text{moles of sodium cyanoborohydride}} \quad (8)$$

Then, the reaction mixture was stirred for 24 h at 40 °C, then dialyzed against distilled water (Spectra/Por® Standard RC tubing; MWCO 1 kDa) for 24 h and lyophilized.

## 2.8. Characterization of $\text{H}_2\text{N-PEG-GAL}$ derivative

The content of amine-terminated side chains was determined by modified TNBSA assay [14]. A stock solution of  $\text{H}_2\text{N-PEG-GAL}$  (10 mg/ml) was prepared in a borate buffer (0.1 M  $\text{Na}_2\text{B}_4\text{O}_7 \cdot \text{H}_2\text{O}$ , pH 9.3). 25  $\mu\text{l}$  of this solution were added to a cuvette containing 950  $\mu\text{l}$  of borate buffer and 25  $\mu\text{l}$  of 0.03 M TNBSA solution. After 90 min incubation, absorbance at  $\lambda = 500 \text{ nm}$  was measured and compared with that estimated for the reaction of  $\text{H}_2\text{N-PEG-NH}_2$  ( $-\text{NH}_2$  in the range between 0.01 and 0.001 mmol/ml) with TNBSA.

The anthrone–sulfuric acid colorimetric assay was used to determine the content of GAL in  $\text{H}_2\text{N-PEG-GAL}$  derivative [15,16]. Anthrone was dissolved in a mixture sulfuric acid/water 3:1 v/v before use, and then 1.5 ml of this solution was added to 0.5 ml of  $\text{H}_2\text{N-PEG-GAL}$  derivative copolymer dispersion (1 mg/ml). The mixture was kept at 100 °C in hot water for 10 min, then allowed to cool at room temperature and analyzed at  $\lambda = 625 \text{ nm}$ . The calibration curve was constructed based on the various GAL concentrations and their corresponding absorbance determined by spectrophotometer at 625 nm. The concentration of GAL linked onto  $\text{H}_2\text{N-PEG-GAL}$  derivative was calculated from the calibration curve. Each experiment was performed in triplicate. The amount of GAL grafted onto  $\text{H}_2\text{N-PEG-GAL}$  derivative was calculated by the following equation:

$$\text{GAL wt\%} = \left( \frac{\text{measured GAL weight in the sample}}{\text{sample weight}} \right) \times 100 \quad (9)$$

## 2.9. Synthesis of PHEA-RhB-PLA-PEG-GAL graft copolymer

PHEA-RhB-PLA (64 mg/ml) was dissolved in *a*-DMA at 40 °C under argon atmosphere and DEA, as catalyst, and a proper amount of DSC were added, according to  $R_7 = 0.1$  and  $R_8 = 1$ , being:

$$R_8 = \frac{\text{moles of TEA}}{\text{moles of DSC}} \quad (11)$$

The reaction mixture was kept at 40 °C for 4 h and then added to a solution of  $\text{H}_2\text{N-PEG-GAL}$  in *a*-DMA (24 mg/ml) in a such way to have  $R_9 = 0.075$ , being:



The obtained mixture reaction was left at 25 °C for 18 h under argon and continuous stirring, then dialyzed against distilled water (Spectra/Por® Standard RC tubing; MWCO 12–14 kDa) and lyophilized. The product was obtained with a yield of 92 wt% based on the starting PHEA-RhB weight.

## 2.10. Characterization of PHEA-RhB-PLA-PEG-GAL graft copolymer

PHEA-RhB-PLA-PEG-GAL graft copolymer was characterized by <sup>1</sup>H NMR and SEC analyses.

<sup>1</sup>H NMR (300 MHz, DMF-*d*<sub>7</sub>, 25 °C, TMS): δ 1.15 (m, 12H<sub>RhB</sub> CH<sub>3</sub>–CH<sub>2</sub>–); δ 1.45 and δ 1.86 (2d, 582 H<sub>PLA</sub> –O–CO–CH(CH<sub>3</sub>)–O–); δ 2.9 (m, 2H<sub>PHEA</sub> –CO–CH–CH<sub>2</sub>–CO–NH–); δ 3.49 (t, 2H<sub>PHEA</sub> –NH–CH<sub>2</sub>–CH<sub>2</sub>–O–); δ 3.71 (t, 2H<sub>PHEA</sub> –NH–CH<sub>2</sub>–CH<sub>2</sub>–O–); δ 3.77 (t, 176 H<sub>PEG</sub> –CH<sub>2</sub>–CH<sub>2</sub>–O–); δ 4.3–4.6 and δ 5.3–5.50 (m, 194 H<sub>PLA</sub> –O–CO–CH(CH<sub>3</sub>)–), and δ 5.0 (m, 1H<sub>PHEA</sub> –NH–CH(CO)CH<sub>2</sub>–); δ 7.0–8.0 (m, 10H<sub>RhB</sub> H–Ar).  $\bar{M}_w$  of PHEA-RhB-PLA-PEG-GAL graft copolymer, determined by SEC analysis, was found to be 100.0 kDa ( $\bar{M}_w/\bar{M}_n = 1.38$ ).

## 2.11. Synthesis of PHEA-RhB-PLA-PEG copolymer

PHEA-RhB-PLA (65 mg/ml) was dissolved in *a*-DMA at 40 °C under argon atmosphere and then DEA and a proper amount of DSC were added according to equations (10) and (11). The reaction mixture was kept at 40 °C for 4 h and then added to a solution of H<sub>2</sub>N-PEG-OCH<sub>3</sub> in *a*-DMA (12 mg/ml) in a such way to have R<sub>10</sub> = 0.075, being:

$$R_{10} = \frac{\text{moles of } -\text{NH}_2 \text{ on H}_2\text{N} - \text{PEG} - \text{OCH}_3}{\text{moles of hydroxyl} - \text{carrying PHEA} - \text{RhB} - \text{PLA repeating units}} \quad (13)$$

The obtained mixture reaction was left at 25 °C for 18 h under argon and continuous stirring, then dialyzed against distilled water (Spectra/Por® Standard RC tubing; MWCO 12–14 kDa) and lyophilized. The product was obtained with a yield of 95wt% based on the starting PHEA-RhB.

## 2.12. Characterization of PHEA-RhB-PLA-PEG graft copolymer

PHEA-RhB-PLA-PEG graft copolymer was characterized by <sup>1</sup>H NMR and SEC analyses.

<sup>1</sup>H NMR (300 MHz, DMF-*d*<sub>7</sub>, 25 °C, TMS): δ 1.15 (m, 12H<sub>RhB</sub> CH<sub>3</sub>–CH<sub>2</sub>–); δ 1.48 and δ 1.96 (2d, 582 H<sub>PLA</sub> –O–CO–CH(CH<sub>3</sub>)–O–); δ 3.0 (m, 2H<sub>PHEA</sub> –CO–CH–CH<sub>2</sub>–CO–NH–); δ 3.48 (t, 2H<sub>PHEA</sub> –NH–CH<sub>2</sub>–CH<sub>2</sub>–O–); δ 3.71 (t, 2H<sub>PHEA</sub> –NH–CH<sub>2</sub>–CH<sub>2</sub>–O–); δ 3.78 (t, 176 H<sub>PEG</sub> –CH<sub>2</sub>–CH<sub>2</sub>–O–); δ 4.3–4.6 and δ 5.3–5.6 (m, 194 H<sub>PLA</sub> –O–CO–CH(CH<sub>3</sub>)–), and δ 5.0 (m, 1H<sub>PHEA</sub> –NH–CH(CO)CH<sub>2</sub>–); δ 7.0–8.0 (m, 10H<sub>RhB</sub> H–Ar).  $\bar{M}_w$  of PHEA-RhB-PLA-PEG-GAL graft copolymer, determined by SEC analysis, was found to be 101.4 kDa ( $\bar{M}_w/\bar{M}_n = 1.31$ ).

## 2.13. Nanoparticle preparation

Fluorescent polymeric nanoparticles were prepared starting from PHEA-RhB-PLA-PEG-GAL (GAL-FNPs) or PHEA-RhB-PLA-PEG (FNPs) by high pressure homogenization-solvent evaporation method [11]. The organic phase was prepared by dispersing each copolymer (17 mg/ml) in dichloromethane (4 ml). This organic

solution was added to 50 ml of an aqueous phase and a primary o/w emulsion was obtained by using an Ultra-Turrax (T 25, Janke & Kunkel Ika – Labortechnik) at 13,500 rpm. This emulsion was diluted by 25 ml of twice-distilled water and then broken down into nano-droplets by applying external energy (7500 psi, through a homogenizer) for one cycle by using an EmulsiFlex™-C5 high pressure homogenizer (Avestin Inc., Canada), equipped with Totem CCS 338 (FIAC, Italy) air compressor. Then, the extraction of the solvent was achieved by evaporation under reduced pressure. As a consequence of this extraction the polymer precipitated leading to the formation of nanoparticles, which were dialyzed against twice-distilled water and, after addition of glycerol as cryoprotectant (nanoparticle/cryoprotectant weight ratio = 5.5), dried by using a Modulyo freeze-dryer (Labconco Corporation, Missouri, U.S.A.). The recovered solid product was stored in freezer for further characterization.

## 2.14. Dimensional analysis and ζ potential measurements

The mean diameter (by number distribution) and width of distribution measurements were performed by photon correlation spectroscopy (PCS) by using the Zetasizer Nano ZSP (Malvern Instrument, Malvern). The measurements were carried out at a fixed angle of 173° and at 25 °C by using filtered isotonic phosphate buffered saline (PBS) aqueous solution at pH 7.4 as suspending medium. Each dispersion was kept in a cuvette and analyzed in triplicate.

ζ potential values were measured using principles of laser doppler velocitometry and phase analysis light scattering (M3-PALS

technique) by dispersing samples in filtered isotonic PBS aqueous solution at pH 7.4, and by analyzing them in triplicate.

## 2.15. Transmission electron microscopy (TEM) analysis

TEM micrographs were acquired by using a JEM-2100 (JEOL, Japan) electron microscope, operating at a 200 kV accelerating voltage. A few tens of a milligram of the freeze-dried samples were dispersed in 2 ml of bi-distilled water and a small drop of the dispersion was deposited on a 300 mesh carbon-coated copper grid, which was introduced into the TEM analysis chamber after complete solvent evaporation.

## 2.16. Chemical and enzymatic stability

The chemical and enzymatic stability of ester linkage between RhB and copolymer was studied in different incubation media and in sink conditions by evaluating the release of RhB by a dialysis method.

To evaluate gastric stability, a fluid simulating conditions in the stomach in the fasted state (FaSSGF) was used by preparing a solution of NaCl (30 mM), pepsin (0.1 mg/ml), sodium taurocholate (80 μM) and lecithin (20 μM), at pH 1.6 by addition of HCl [10,17]. To evaluate intestinal stability, a fluid simulating the proximal small intestine conditions in fasted state (FaSSIF) was used by preparing a solution of monobasic potassium phosphate (3.9 g/l), KCl (7.7 g/l), sodium taurocholate (3 mM) and lecithin (0.75 mM), at pH 6.5 by addition of NaOH [10,18]. To evaluate stability in physiological

buffers, phosphate buffered saline (PBS, NaCl, Na<sub>2</sub>HPO<sub>4</sub>, KH<sub>2</sub>PO<sub>4</sub>) at pH 7.4 or at pH 5.5 were used as suspending media. To evaluate enzymatic stability, PBS aqueous dispersions containing esterase from porcine liver or lipase from porcine pancreas type II (final theoretical ratio between the esterase activity of enzyme and ester groups between RhB and the polymeric backbone ~100) were used as suspending media.

GAL-FNPs sample was dispersed in the proper medium (2 ml), placed in a dialysis bag (Spectra/Por® Standard RC tubing; MWCO 12–14 kDa) immersed in the same medium, and then incubated in a thermostatic orbital shaker (100 rpm, 37 °C). At scheduled time-points (1, 2, 4, 6, 24 h and 4 days), aliquots of the receiver medium was taken and replaced by fresh medium. A control experiment was also performed by carrying out the same experiments on an appropriate amount of PHEA-RhB. The released RhB amounts in the receiver medium were determined by the HPLC method described below.

### 2.17. RhB HPLC analysis

The amount of RhB released in the receiver medium was determined by an HPLC method [19]. The column was a Gemini C18 (μBondpack, 5 μm, 250 × 46 mm i.d., obtained from Waters); the mobile phase was a mixture of aqueous solution of NaC<sub>7</sub>H<sub>15</sub>SO<sub>3</sub> (5 mM):CH<sub>3</sub>CN:MeOH 20:45:35 (v:v:v) with a flow rate of 0.8 ml/min, the column temperature was 25 °C, and the detection wavelength was 550 nm. 40 μl sample was injected into the column. The obtained peak area ( $t_r = 3.89$  min) corresponding to free RhB was compared with a calibration curve obtained by plotting areas versus standard solution concentrations of RhB in twice-distilled water in the range of 5–0.1 μg/ml ( $y = 9E + 10^8x$ ,  $R^2 = 0.9998$ ). Results were expressed as the weight percent ratio between the released RhB and the total amount initially covalently linked to the incubated sample (nanoparticles or PHEA-RhB).

### 2.18. Physical stability

Physical stability of GAL-FNPs or FNPs aqueous dispersion was studied in PBS by monitoring the mean size (by number distribution), width of distribution and ζ potential values as a function of incubation time until 24 h.

Each nanoparticle sample was dispersed in PBS and incubated in a thermostatic compartment at 37 °C. At scheduled time-points (2, 5, 7 and 24 h), aliquots were kept in a cuvette and analyzed in triplicate as described above.

### 2.19. Cell culture

Human hepatocellular carcinoma (HepG2) and human cervical carcinoma (HeLa) cells were cultured in DMEM supplemented with 10 vol% FBS and antibiotics (Gibco-Life Technology).

### 2.20. Cell viability assay

HepG2 and HeLa cells seeded respectively at  $12 \times 10^3$  and  $24 \times 10^3$  cells/cm<sup>2</sup>, were treated with different concentration (from 0.1 to 0.5 mg/ml) of GAL-FNPs or FNPs, and viability was determined after 24 h, 48 h and 72 h through WST1 assay (Roche) following manufacturer's instructions.

### 2.21. Confocal analysis of HepG2 and HeLa cells exposed to nanoparticles

To evaluate the cellular uptake of GAL-FNPs or FNPs, these were suspended at 250 μg/ml in DMEM, 0.5 vol% FBS, and then added to

the cell culture wells (HepG2 or HeLa). After incubation at 37 °C for 1, 3, or 5 h, the cells were washed, fixed with 4 vol% para-formaldehyde in PBS at room temperature, treated with Alexa Fluor® 488 Phalloidin to stain the cytoskeleton and with DAPI to stain the nuclei. Confocal analysis was performed with TCS-SP8 (Leika).

### 2.22. Statistical analysis

All the experiments were repeated at least three times. All data are expressed as means ± standard deviation. All data were analyzed by Student's *t*-test. A *p*-value <0.05 was considered as statistically significant, while a *p*-value <0.01 was considered as highly significant.

## 3. Results and discussion

In this paper, the synthesis of an amphiphilic graft copolymer starting from α,β-poly(*N*-2-hydroxyethyl)-D,L-aspartamide (PHEA) and bearing rhodamine B (RhB) moieties, polylactide (PLA) and galactosylated polyethylene glycol (PEG) chains, is described. Then, its use for the preparation of galactosylated polymeric fluorescent nanoparticles (GAL-FNPs) for in vitro imaging applications is reported in detail.

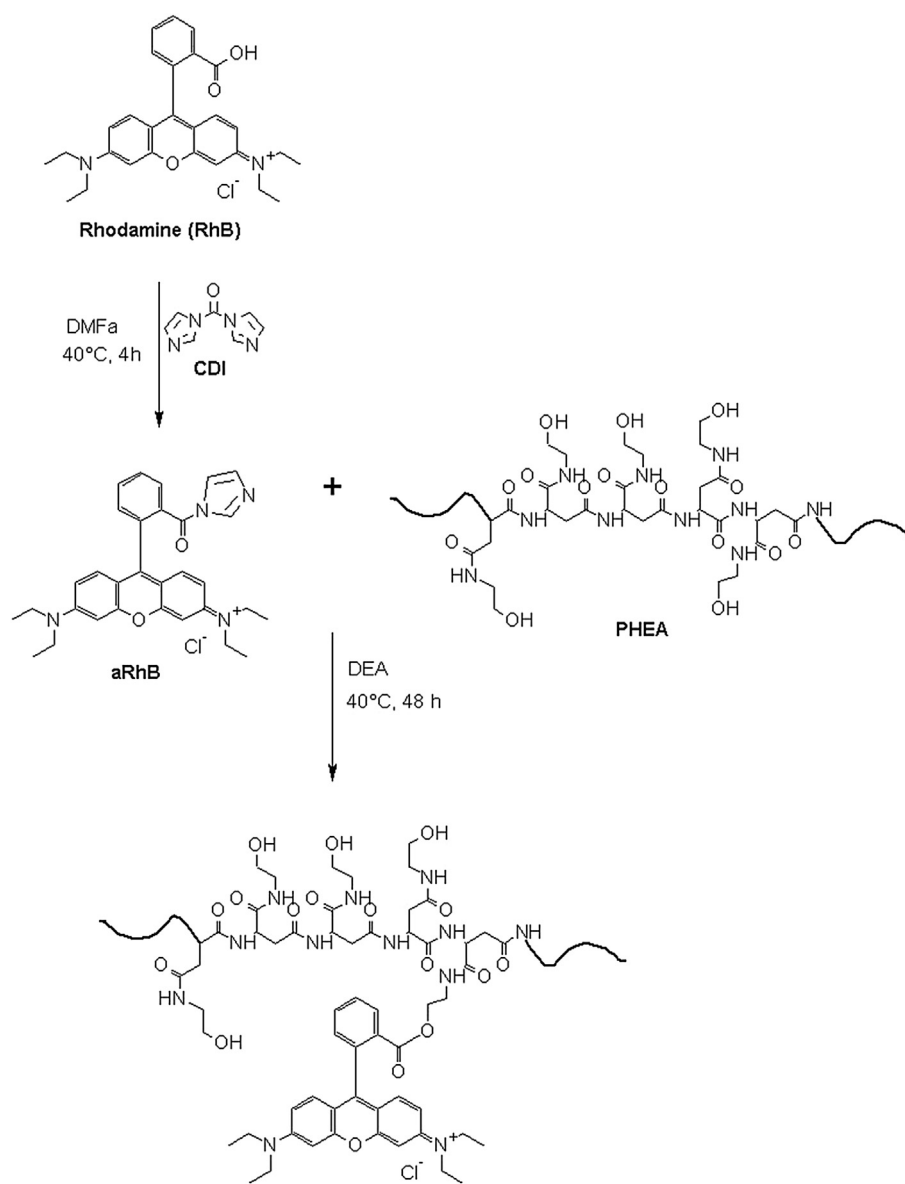
The derivatization of PHEA with these three functionalities has different aims. First, the derivatization of PHEA with RhB could be potentially a valid approach to introduce a fluorescent probe permanently conjugated on the polymeric backbone with high potential in imaging. As a consequence, it could be possible to follow the fate of either the copolymer or obtained copolymer-based nanostructured systems in vitro and in vivo [20–22]. Second, the grafting of PLA to PHEA-RhB, which is still a highly water soluble polymer such as PHEA, enables to modify its structural and functional properties. In particular, PLA chains allow to introduce on PHEA-RhB biodegradable hydrophobic chains that give amphiphilic properties to the resulting copolymer to make it suitable for preparing polymeric nanoparticles. Third, the derivatization of PHEA-RhB-PLA with -PEG-GAL residues allow to obtain a polymeric conjugate targeted to hepatocytes. Moreover, PEG chains, introduced as a spacer between PHEA-RhB-PLA and galactose (GAL) molecules, could allow the best interaction of the targeting moieties with their receptors in vivo, thanks to their chain flexibility.

### 3.1. Synthesis and characterization of PHEA-RhB-PLA-PEG-GAL graft copolymer

The first synthetic step was the covalent linkage of RhB on PHEA. RhB was chosen as fluorescent probe because of high absorption coefficient, photo-stability and other properties of rhodamine dyes so that many strategies were recently developed in order to covalently link them to biomolecules, polymers and surfaces [23,24].

To obtain a fluorescent derivative of PHEA, the first reaction step was the derivatization of PHEA with RhB to obtain PHEA-RhB, by using carbonyldiimidazole (CDI) as coupling agent and reactive amounts in according to equations (1)–(3). The synthetic procedure and chemical structure of PHEA-RhB copolymer is reported in Scheme 1. The obtained product was soluble in water, dimethylsulfoxide, dimethylformamide, such as starting PHEA.

The degree of derivatization of PHEA-RhB copolymer in RhB molecules ( $DD_{RhB}$ ) was calculated from the <sup>1</sup>H NMR spectrum in D<sub>2</sub>O by comparing the integral of the peaks related to protons between δ 7.90–8.60 ( $H = 10$ ), attributed to protons of RhB aromatic rings to the integral related to protons at δ 3.32 attributed to –NH–CH<sub>2</sub>–CH<sub>2</sub>–O– (belonging to PHEA). The  $DD_{RhB}$  was expressed as mean values of three determinations and resulted to



**Scheme 1.** Synthetic procedure of PHEA-RhB copolymer.

be  $0.55 \pm 0.05$  mol% of repeating units. By proper calculation it is possible to determined that  $DD_{RhB}$  corresponds to about 1–2 RhB molecules for each PHEA chain. The confirmation that the RhB molecules were chemically linked to the polymer was obtained by HPLC analysis that revealed the absence of free RhB in the isolated product (data not shown). The  $\bar{M}_w$  of PHEA-RhB copolymer results to be equal to 35 kDa with a  $\bar{M}_w/\bar{M}_n$  of 1.41; this apparently reduced  $\bar{M}_w$  value of PHEA-RhB compared to that of PHEA could be attributed to a modification of the PHEA conformation due to the linkage of RhB.

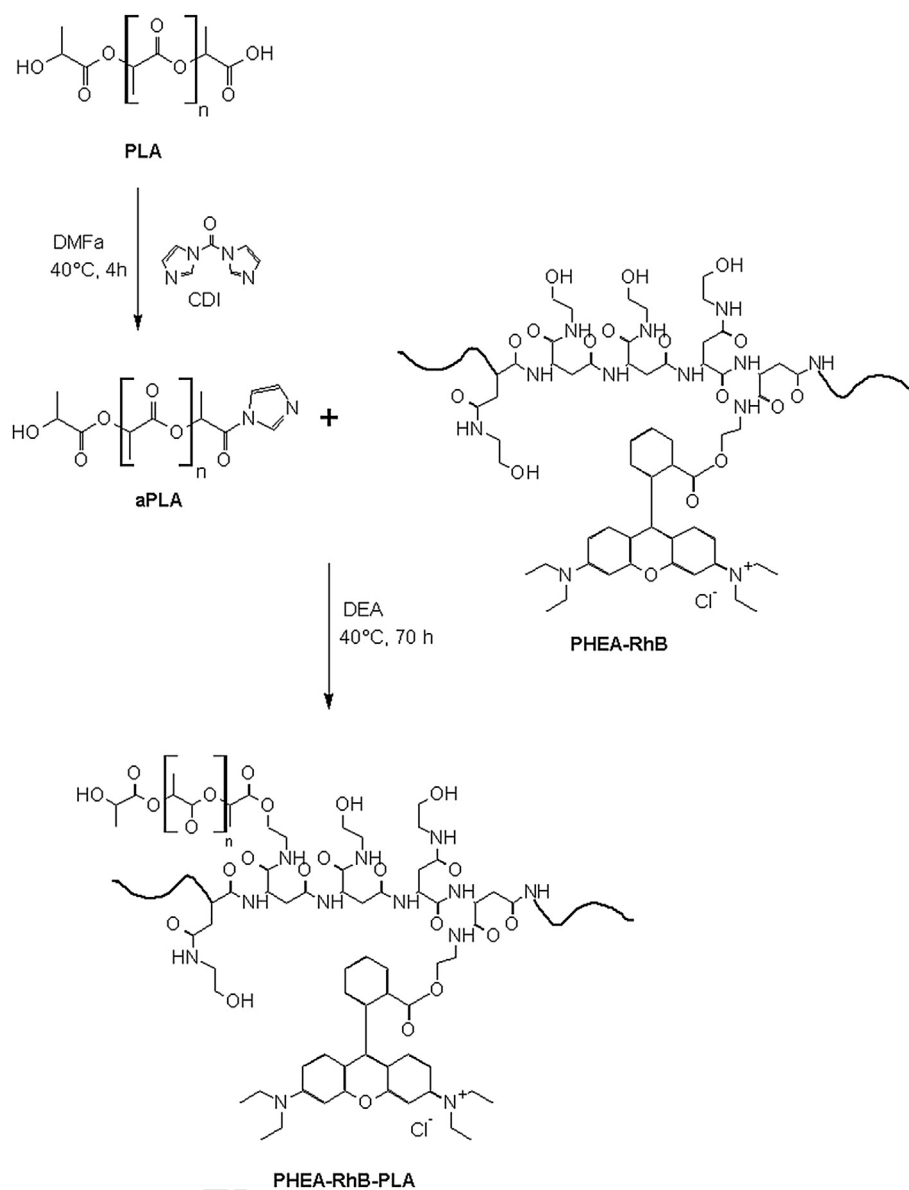
Being well known from the literature that the conjugation of RhB to molecules or polymers could cause the shift of the maxima wavelength, the reduction of molar extinction coefficient ( $\epsilon$ ) of the obtained derivative or the total fluorescence disappearance [25], either maximum wavelength or  $\epsilon$  values of PHEA-RhB were determined and compared to that of RhB aqueous solutions by recording UV–vis spectra. It was found that the maximum wavelength was shift from 554 nm to 561 nm starting from RhB to PHEA-RhB, and  $\epsilon$  resulted to be  $117,000 \text{ M}^{-1} \text{ cm}^{-1}$  for RhB (in accordance with data

reported in the literature) and  $53,200 \text{ M}^{-1} \text{ cm}^{-1}$  for PHEA-RhB [25]. However, although this latter is halved than that of RhB, this value is still high to confer fluorescence properties to PHEA-RhB derivatives.

Then, in order to allow the grafting of acid terminated PLA onto PHEA-RhB, the carboxyl groups of PLA were activated for 4 h by using CDI as coupling agent. Then, the activated PLA (aPLA) was left to react with hydroxyl side groups on PHEA for 70 h, in organic environment at 40 °C, with PLA, CDI and DEA amounts calculated in according to equations (4)–(6). The synthetic procedure and chemical structure of PHEA-RhB-PLA copolymer is reported in Scheme 2.

Thanks to the introduction of hydrophobic PLA chains to the water soluble PHEA-RhB copolymer, the obtained product was insoluble in water, but soluble in dimethylsulfoxide, dimethylformamide and dichloromethane. The  $^1\text{H}$  NMR spectrum in  $\text{DMF-d}_7$  of PHEA-RhB-PLA graft copolymer is reported in Fig. 1a.

The degree of derivatization of PHEA-RhB-PLA graft copolymer in PLA chains ( $DD_{PLA}$ ) was calculated by comparing the integral of the



**Scheme 2.** Synthetic procedure of PHEA-RhB-PLA graft copolymer ( $n = 194$ ).

peaks related to protons between  $\delta$  1.40–1.80 ( $H = 582$ ) as well as to protons ( $H = 194$ ) between  $\delta$  4.20–4.60 and  $\delta$  5.20–5.90 (assigned to  $-\text{O}-\text{CO}-\text{CH}(\text{CH}_3)-\text{O}-$  and  $-\text{O}-\text{CO}-\text{CH}(\text{CH}_3)-$  belonging to linked PLA chains), respectively, to the integral related to protons at  $\delta$  5.00 attributed to  $-\text{NH}-\text{CH}(\text{CO})\text{CH}_2-$ . The  $\text{DD}_{\text{PLA}}$  was expressed as mean value of three determinations and resulted to be  $1.9 \pm 0.2$  mol% of repeating units. By proper calculation it can be found that there are about 4 PLA molecules for each PHEA-RhB chain.

The functionalization by PLA chains was confirmed by data obtained by SEC analysis (see experimental part). The  $\overline{M}_w$  of PHEA-RhB-PLA copolymer results to be equal to 86.9 kDa with a  $\overline{M}_w/\overline{M}_n$  of 1.45. This value is in accordance with the theoretical values calculated for PHEA-RhB-PLA copolymer, considering the starting PHEA  $\overline{M}_w$  and the resulting DD values in RhB and PLA, respectively (see Table 1). Moreover, this value also demonstrated that no degradation phenomena occurred in PHEA-RhB copolymer due to the reaction conditions chosen for obtaining PHEA-RhB-PLA graft copolymer.

At the same time, in order to obtain a reactive that could be used to introduce GAL residues and hydrophilic portions on PHEA-RhB-PLA backbone, a galactosylated derivative of poly(ethylene glycol), the O-(2-aminoethyl)-O'-galactosyl poly(ethylene glycol) (GAL-PEG-NH<sub>2</sub>) was obtained by a reductive amination of lactose with primary amine functions of poly(ethylene glycol)bis(amine) (H<sub>2</sub>N-PEG-NH<sub>2</sub>) in the presence of sodium cyanoborohydride, in experimental conditions to obtain about the galactosylation of about half amine groups. The synthetic procedure and chemical structure of H<sub>2</sub>N-PEG-GAL is reported in Scheme 3.

After purification by exhaustive dialysis, the degree of free  $-\text{NH}_2$  was measured by evaluating directly the free amine-terminated side chains by modified TNBSA colorimetric assay and indirectly the N-substitution of H<sub>2</sub>N-PEG-NH<sub>2</sub> by GAL by anthrone-sulfuric acid colorimetric method [14,16]. The mole percent of free  $-\text{NH}_2$  groups, expressed as percent ratio between the free amine groups and the total amine groups on H<sub>2</sub>N-PEG-NH<sub>2</sub>, was found to be  $32.0 \pm 6.1$  mol%.



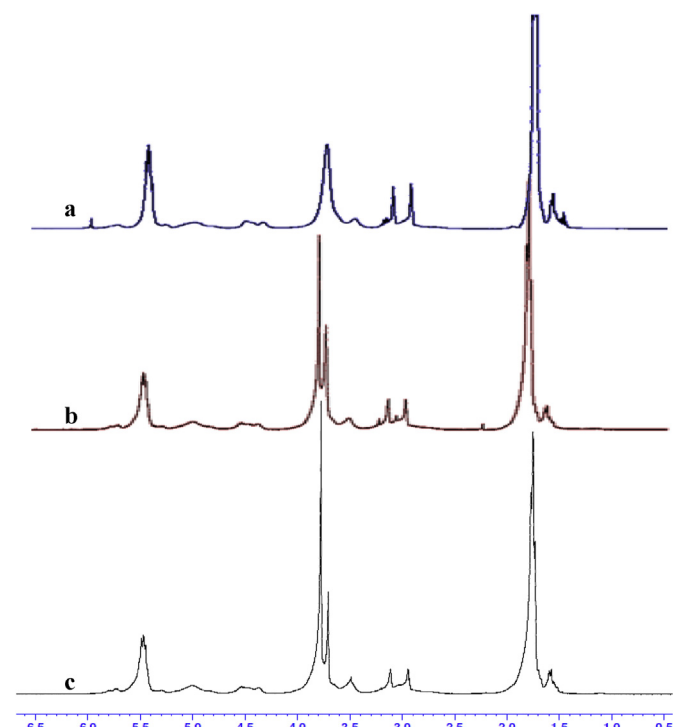


**Fig. 1.**  $^1\text{H}$  NMR spectra of copolymers: PHEA-RhB-PLA (a), PHEA-RhB-PLA-PEG-GAL (b), PHEA-RhB-PLA-PEG (c) in  $\text{DMF-}d_7$ .

Then, the obtained  $\text{H}_2\text{N-PEG-GAL}$  was grafted on PHEA-RhB-PLA to obtain PHEA-RhB-PLA-PEG-GAL copolymer by activating the free  $-\text{OH}$  on PHEA-RhB-PLA via disuccinimidyl carbonate (DSC) and by using TEA as catalyst, in organic environment.

In particular, a theoretical ratio between the free amine-terminated in  $\text{H}_2\text{N-PEG-GAL}$  side chains and the hydroxyl-carrying PHEA-RhB-PLA repeating units ( $R_0$ ) was fixed equal to 0.075, while the employed amounts of DSC and TEA were defined by equations (10) and (11). The probability of a competitive occurrence of terminal  $-\text{OH}$  activation in PLA chains with DSC and subsequent reaction with  $\text{H}_2\text{N-PEG-GAL}$  is considered low due to the DD in PLA of  $-\text{OH}$  repeating units of PHEA.

The synthetic procedure and chemical structure of PHEA-RhB-PLA-PEG-GAL graft copolymer is also reported in Scheme 3, while the  $^1\text{H}$  NMR in  $\text{DMF-}d_7$  in Fig. 1b.

The degree of derivatization in  $\text{PEG}_{2000}$  chains ( $\text{DD}_{\text{PEG}}$ ) was calculated by comparing the integral of the peak related to protons ( $H = 176$ ) at  $\delta$  3.77 attributed to  $-\text{CH}_2-\text{CH}_2-\text{O}-$  (belonging to  $\text{PEG}_{2000}$ ) with the integral related to protons ( $H = 2$ ) a  $\delta$  3.50 attributed to  $-\text{NH}-\text{CH}_2-\text{CH}_2-\text{O}-$  (belonging to PHEA), according to the method reported elsewhere [11,26]. The  $\text{DD}_{\text{PEG}}$  resulted to be  $4.5 \pm 0.5$  mol%. The derivatization degree in GAL moieties was also measured by using the anthrone–sulfuric acid method, which confirmed that the grafting of each PEG chain introduced a GAL molecule on PHEA-RhB-PLA.

At the same time, in order to obtain fluorescent nanoparticles to be used as control in further experiments, a pegylated derivative of PHEA-RhB-PLA was synthesized by following the procedure reported in the experimental part [27]. The chemical structure of PHEA-RhB-PLA-PEG graft copolymer is also reported in Fig. 2. The  $\text{DD}_{\text{PEG}}$ , calculated from the  $^1\text{H}$  NMR spectrum (reported in Fig. 1c), resulted to be  $5.9 \pm 0.3$  mol%.

To properly characterize the obtained copolymers such as PHEA-RhB-PLA-PEG-GAL and PHEA-RhB-PLA-PEG from the molecular point of view, the  $\overline{M}_w$  and the  $\overline{M}_w/\overline{M}_n$  values were determined by SEC analysis; obtained values were also reported in Table 1. These values result to be equal to 100.0 and 101.4 kDa ( $\overline{M}_w/\overline{M}_n=1.38$  and 1.31) and are in accordance with the theoretical values calculated for PHEA-RhB-PLA-PEG-GAL and PHEA-RhB-PLA-PEG copolymers, considering the starting PHEA-RhB-PLA  $\overline{M}_w$  and the resulting DD values in PEG derivatization. Moreover, these values also demonstrated that no degradation phenomena occurred in PHEA-RhB-PLA copolymer backbone due to the reaction conditions chosen for obtaining PHEA-RhB-PLA-PEG-GAL and PHEA-RhB-PLA-PEG graft copolymers, respectively.

### 3.2. Preparation and characterization of fluorescent nanoparticles (FNPs)

Due to the amphiphilic properties of PHEA-RhB-PLA-PEG-GAL and PHEA-RhB-PLA-PEG graft copolymers, polymeric fluorescent nanoparticles (GAL-FNPs and FNPs, respectively) with small size and low width of distribution were easily obtained by the high pressure homogenization (HPH)-solvent evaporation method and by avoiding the use of different surfactants or other emulsion-stabilizing agents, requested normally for nanoparticle production [11,28]. The complete process of nanoparticle production is schematically described in Scheme 4.

In particular, a primary o/w emulsion was obtained by addition of the copolymer organic solution to an aqueous phase (step 1 of Scheme 4), which was diluted and subjected to HPH (step 2). Then, the extraction of the organic solvent under reduced pressure allows the polymer precipitation and the formation of galactosylated (GAL-FNPs) or not (FNPs) nanoparticles (step 3), that were freeze-dried in the presence of a cryoprotectant (step 4). The absence of degradation phenomena that could occur on both graft copolymer backbones and/or side chains due to the chosen experimental conditions was confirmed by SEC analysis, as reported for similar copolymers [11].

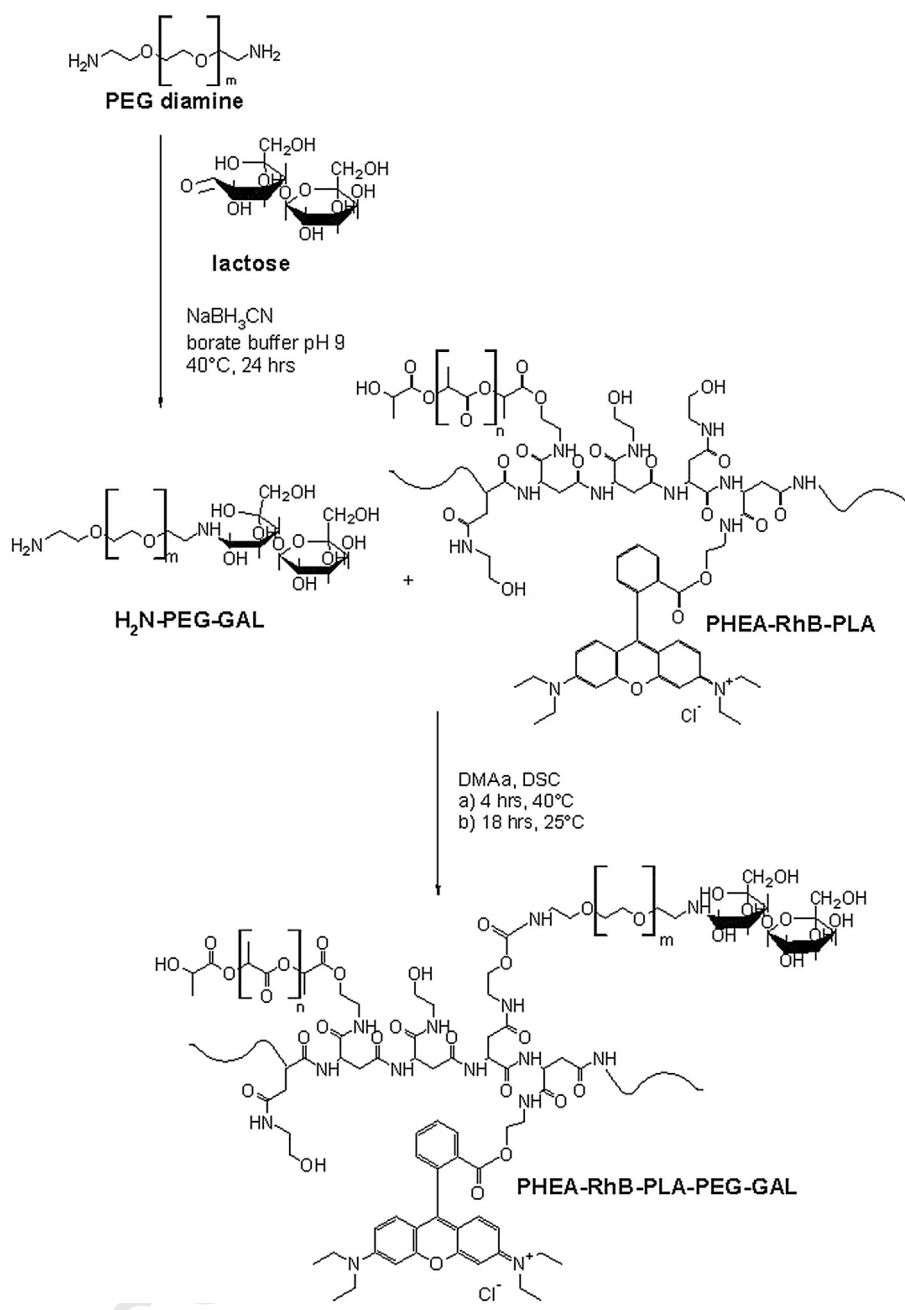
After re-dispersion in a proper medium, GAL-FNPs and FNPs were characterized in terms of mean size (by number distribution), width of distribution and  $\zeta$  potential in phosphate buffer saline (PBS) aqueous solution at pH 7.4 by using Photon Correlation Spectroscopy (PCS). Analytical data are reported in Fig. 3.

Obtained GAL-FNPs show nanoscaled size in isotonic media, with a mean size equal to  $103.1 \pm 43.8$  nm, slightly negative  $\zeta$  potential ( $-3.18 \pm 0.25$  mV) and spherical shape, as showed by TEM images reported in Fig. 4.

These low values in surface charge could be attributed probably to the presence of linked PEG-GAL chains onto the nanoparticle

**Table 1**  
Chemical composition, weight-average molecular weight ( $\overline{M}_w$ ) and polydispersity index ( $\overline{M}_w/\overline{M}_n$ ) of obtained copolymers.

Copolymer	$\text{DD}_{\text{RhB}}$ (mol%) ( $\pm$ S.D.)	$\text{DD}_{\text{PLA}}$ (mol%) ( $\pm$ S.D.)	$\text{DD}_{\text{PEG}}$ (mol%) ( $\pm$ S.D.)	$\overline{M}_w$ (kDa)	$\overline{M}_w/\overline{M}_n$
PHEA	—	—	—	38.0	1.62
PHEA-RhB	$0.55 \pm 0.05$	—	—	35.0	1.41
PHEA-RhB-PLA	$0.55 \pm 0.05$	$1.9 \pm 0.2$	—	86.9	1.45
PHEA-RhB-PLA-PEG-GAL	$0.55 \pm 0.05$	$1.9 \pm 0.2$	$4.5 \pm 0.5$	100.0	1.38
PHEA-RhB-PLA-PEG	$0.55 \pm 0.05$	$1.9 \pm 0.2$	$5.9 \pm 0.3$	101.4	1.31



**Scheme 3.** Synthetic procedure of PHEA-RhB-PLA-PEG-GAL graft copolymer ( $n = 194$ ,  $m = 44$ ).

surface that gives a more shielded surface. In fact, these values were significantly higher when nanoparticles were obtained by using non-pegylated copolymers, as reported elsewhere [11].

FNPs show mean size (by number distribution), width of distribution and surface charge not significantly different from the galactosylated systems, being respectively equal to  $100.3 \pm 52.3$  nm, and  $-3.09 \pm 0.41$  mV.

### 3.3. Chemical and enzymatic stability

In a previous paper, a chemical degradation study on polymeric nanoparticles based on galactosylated and/or pegylated polyaspartamide–polylactic acid copolymers in media mimicking physiological compartments demonstrated that the degradation process of PLA copolymers is faster than that showed by simple PLA

nanoparticles, and that is mainly attributed to the loss of water soluble portions of PLA [29]. In particular, after 14 days of incubation at pH 7.4, the percentage of recovered samples was 81.2 and 79.0 wt%, respectively for galactosylated and pegylated nanoparticles, while the degradation of PLA nanoparticles was lesser than 3 wt% in the same medium.

For the use of GAL-FNPs in fluorescent imaging, it is very important that the fluorescent probe is stably linked to the systems. For this reason, the chemical and enzymatic stability of fluorescent dye covalently linked to the copolymer backbone by ester linkage was investigated in mimicking physiological conditions.

In particular, GAL-FNPs were incubated until 4 days of incubation at 37 °C in PBS at pH 7.4 and at pH 5.5 to mimic physiological conditions [10,30]. To mimic a potential oral administration, this study was also carried out in fasted state simulated gastric fluid

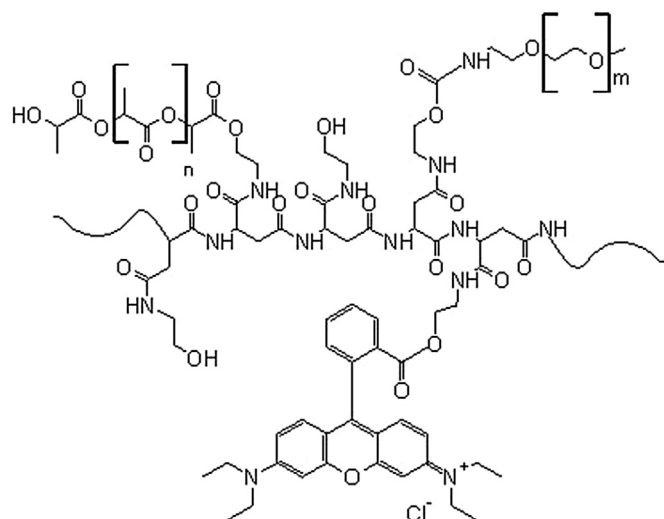


**Fig. 2.** Chemical structure of PHEA-RhB-PLA-PEG graft copolymer ( $n = 194$ ,  $m = 44$ ).

(FaSSGF) at pH 1.6 to mimic gastric conditions, in fasted state simulated intestinal fluid (FaSSIF) at pH 6.5 to mimic intestinal conditions [10,31].

The stability of covalent linkage was determined by evaluating the amount of released RhB from GAL-FNPs at prefixed time intervals across a dialysis tube. For comparison, this experiment was also carried out on PHEA-RhB, to evaluate if the great accessibility of ester linkage between RhB and PHEA in the water-soluble starting copolymer could modify the degradation profile of the covalently linked dye. Moreover, the RhB diffusion profile alone was investigated in each medium in order to determine the diffusion rate of the free drug across the dialysis membrane. The diffusion

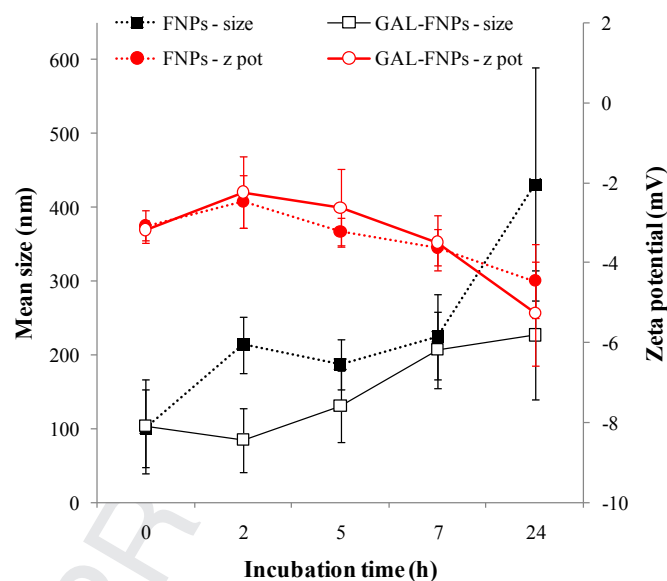
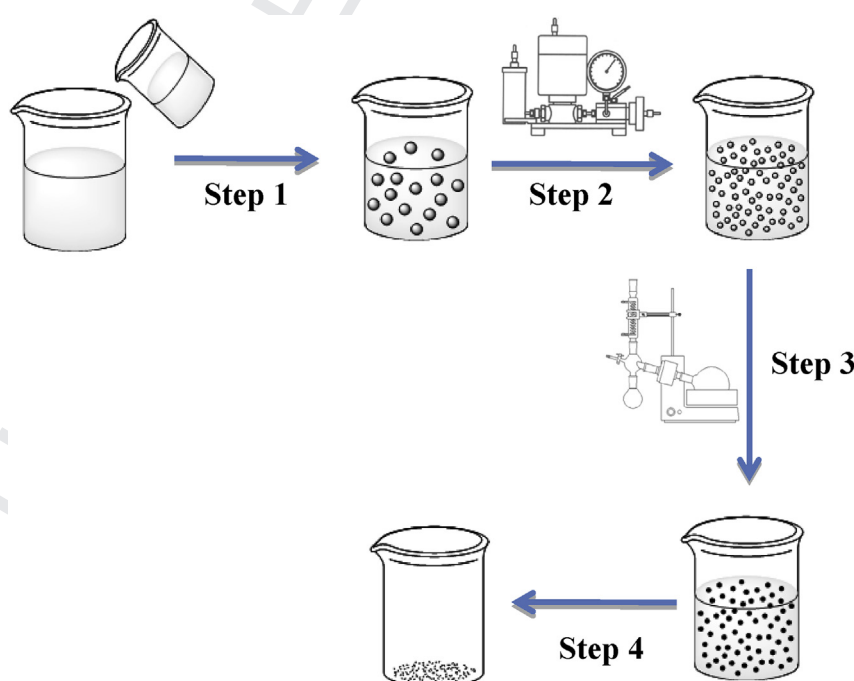


**Fig. 3.** Physical stability of GAL-FNPs and FNPs in PBS at 37 °C. Changes of particle size (by number distribution), width of distribution and  $\zeta$  potential as a function of incubation time.

rate resulted to be very fast, being the free RhB freely soluble in aqueous media (data not shown).

The amount of released RhB was expressed as percentage ratio between the weight of released RhB at the prefixed time and the total amount of RhB linked to the GAL-FNPs or PHEA-RhB copolymer. Fig. 5a and b shows the release profiles of RhB from GAL-FNPs and from PHEA-RhB, incubated in: a) FaSSGF, FaSSIF and PBS at pH 5.5, and b) PBS at 7.4.



**Scheme 4.** Schematic representation of the polymeric nanoparticle preparation through the high pressure homogenization-solvent evaporation method. Step 1: mixing of the polymeric PHEA-RhB-PLA-PEG-GAL organic and aqueous phases and formation of the primary emulsion by vigorous stirring, step 2: high pressure homogenization (7500  $\pm$  2500 psi) and nanoemulsion formation, step 3: evaporation of  $\text{CHCl}_3$  under vacuum and step 4: addition of the cryoprotectant and freeze-drying of the aqueous nanoparticle dispersion.

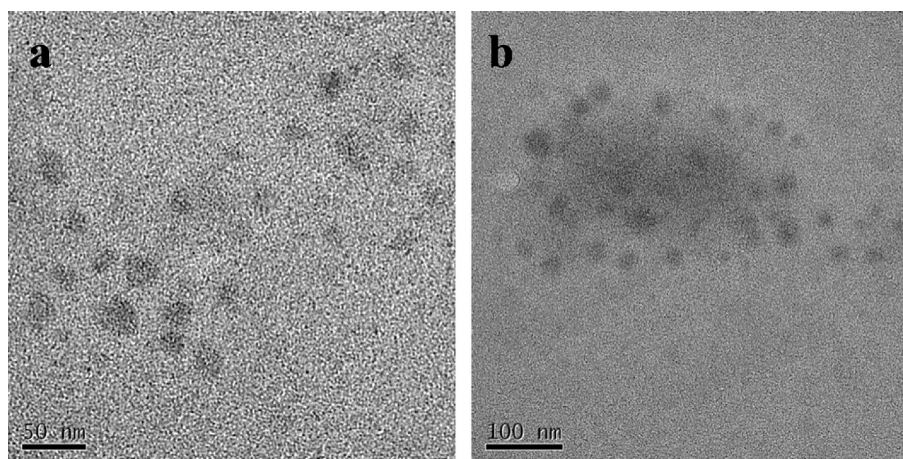


**Fig. 4.** TEM images of GAL-FNPs at two magnifications: a) 50,000 $\times$ , and b) 30,000 $\times$ .

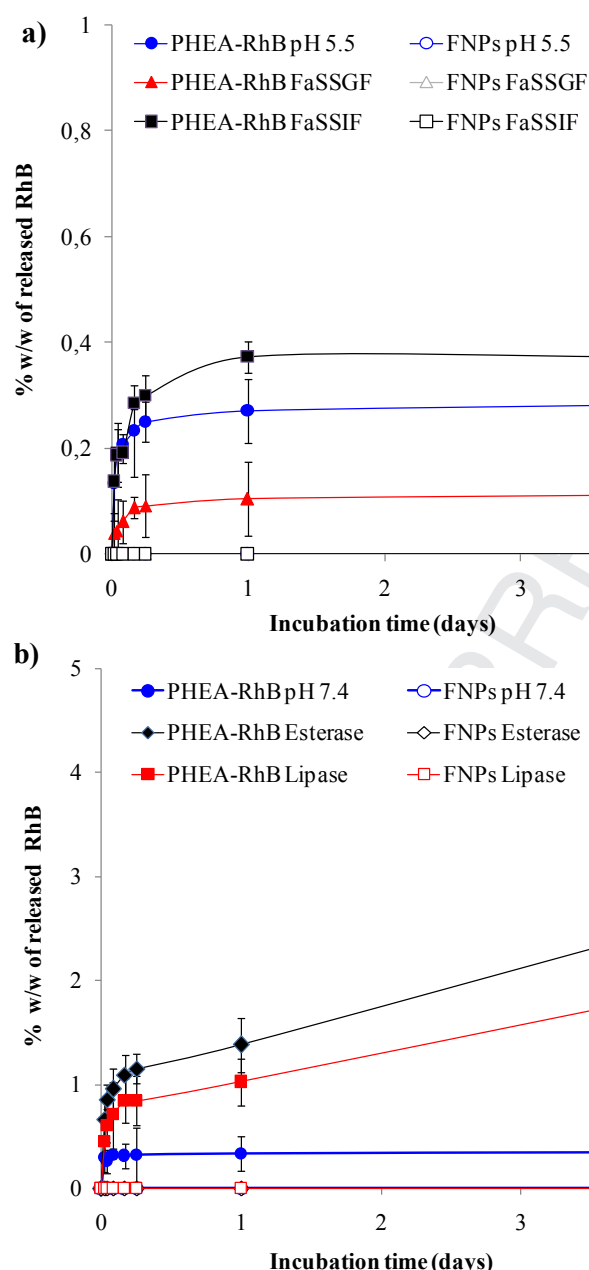


**Fig. 5.** RhB release profiles for 4 days from GAL-FNPs and from PHEA-RhB. Samples were incubated in: a) FaSSGF (pH 1.6), FaSSIF (pH 6.5), PBS at pH 5.5, b) PBS at 7.4, in the absence or in the presence of lipase and esterase enzyme dispersion.

As can be seen, the percentage of RhB released from GAL-FNPs in all investigated media, is almost null until 4 days incubation. For PHEA-RhB, the percentage of degradation was below 0.4 wt% on the total linked amount to the PHEA backbone; although this value is higher than that found for GAL-FNPs, is still very low if compared to the total linked amount to the PHEA backbone.

Enzymatic stability was carried out in the presence of esterase or lipase by following the experimental protocol described for the chemical stability. Obtained results are also reported in Fig. 5b. Also in this case, RhB release from GAL-FNPs is negligible, while that

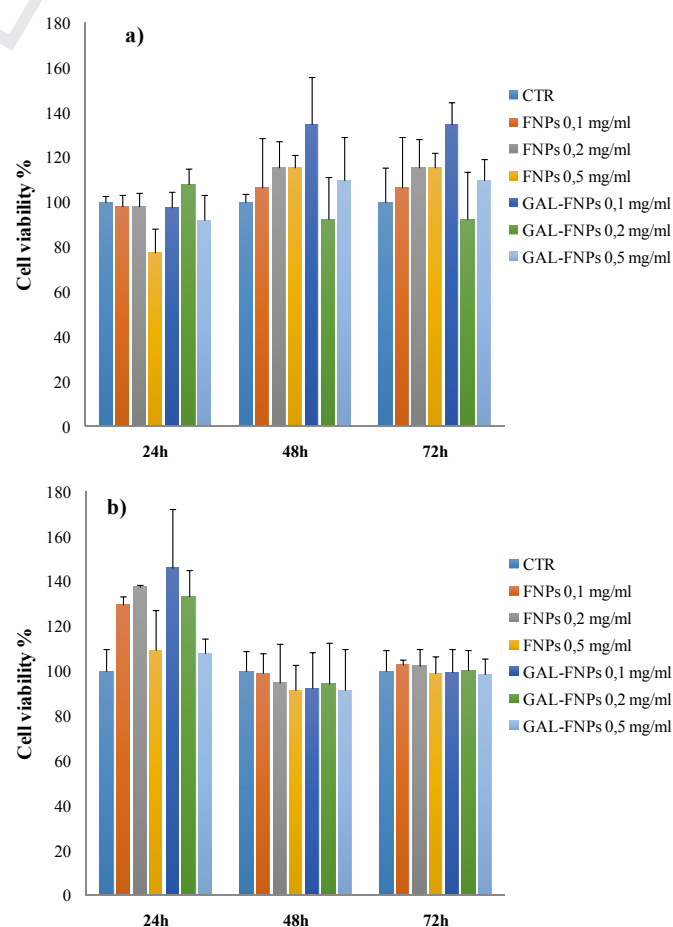


**Fig. 6.** Cell viability assay for: a) HepG2 cells treated with GAL-FNPs and FNPs, b) HeLa cells treated with GAL-FNPs and FNPs. Time points and concentrations are indicated in the figure.



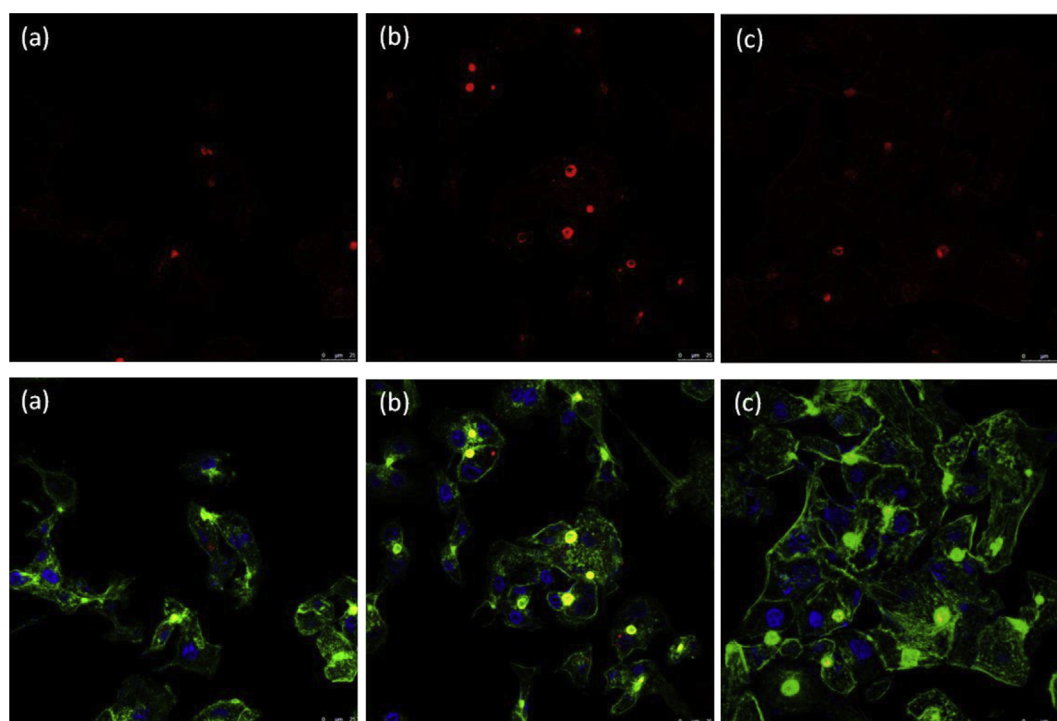


**Fig. 7.** Confocal analysis of HepG2 cells incubated with GAL-FNPs (250 µg/ml) for 1 h (a), 3 h (b), and 5 h (c). In the upper line the GAL-FNPs in red, in the line below the respective merge with DAPI (in blue) and phalloidin (in green). (For interpretation of the references to color in this figure legend, the reader is referred to the web version of this article.)

released from PHEA-RhB was equal to about 2.5 and 1.8 wt% after 4 days incubation, respectively, in the presence of esterase and lipase.

Results of chemical and enzymatic stability could be explained considering that being PHEA-RhB soluble in aqueous media, ester linkage between RhB and PHEA backbone is more accessible by

the enzyme than the same linkage when entrapped into the GAL-FNPs.

Concluding, chemical and enzymatic stability of the ester linkage between fluorescent dye and copolymer backbone forming GAL-FNPs was demonstrated until 4 days of incubation.

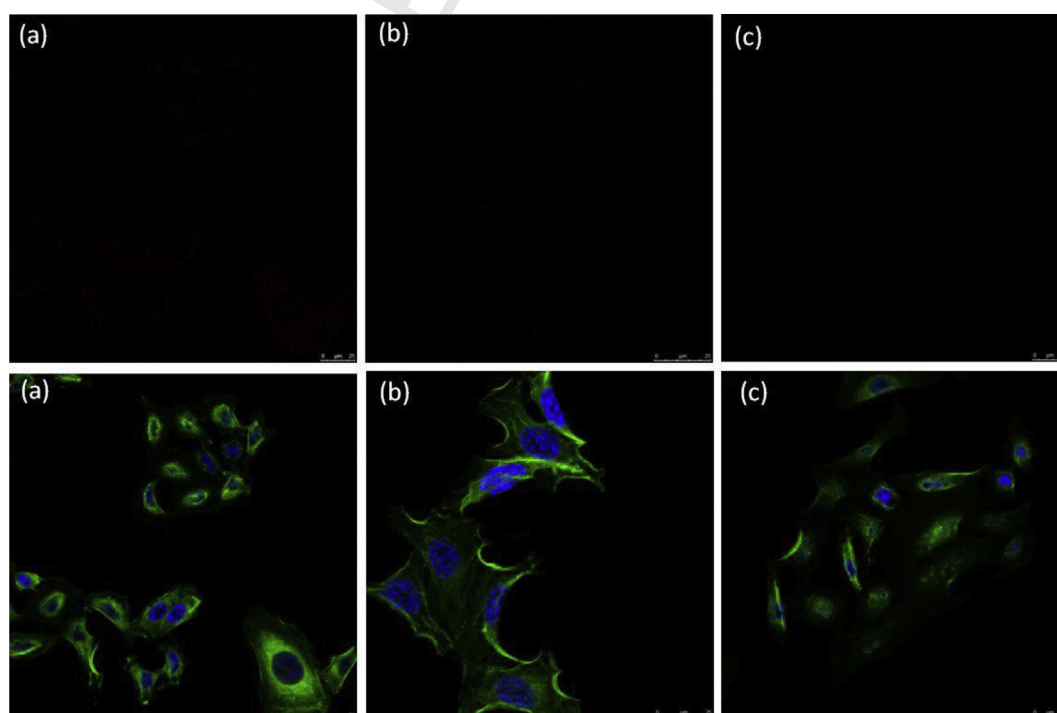


**Fig. 8.** Confocal analysis of HeLa cells incubated with GAL-FNPs (250 µg/ml) for 1 h (a), 3 h (b), and 5 h (c). In the upper line the GAL-FNPs in red, in the line below the respective merge with DAPI (in blue) and phalloidin (in green). (For interpretation of the references to color in this figure legend, the reader is referred to the web version of this article.)

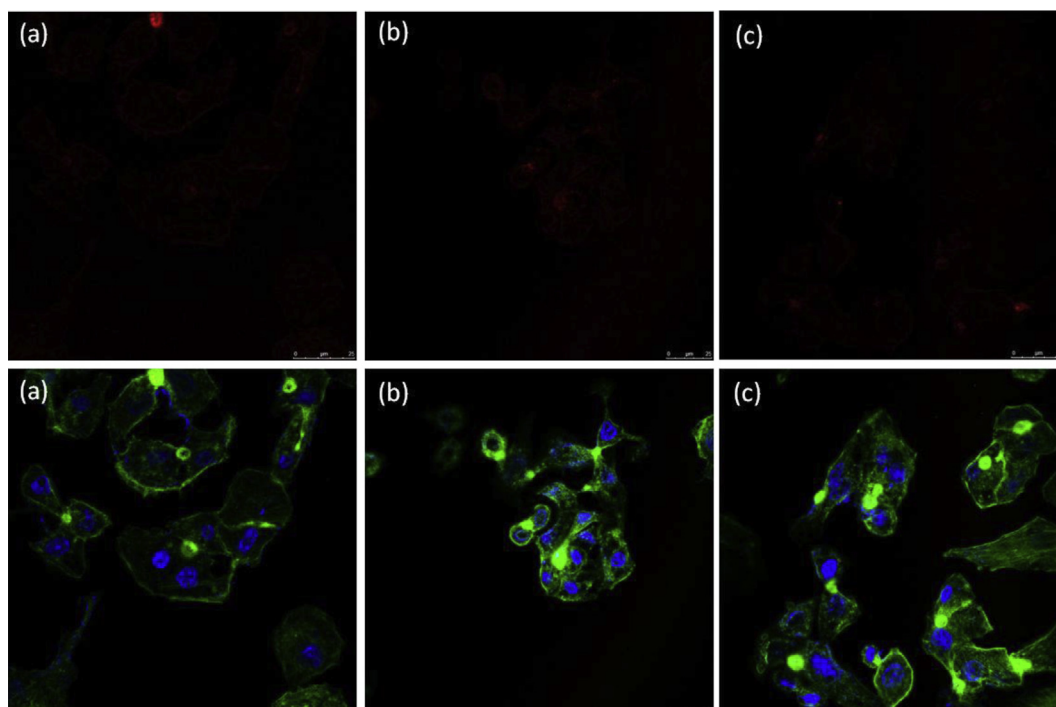


**Fig. 9.** Confocal analysis of HepG2 cells incubated with FNP (250 µg/ml) for 1 h (a), 3 h (b), and 5 h (c). In the upper line the FNP in red, in the line below the respective merge with DAPI (in blue) and phalloidin (in green). (For interpretation of the references to color in this figure legend, the reader is referred to the web version of this article.)

### 3.4. Physical stability

Buffer at pH 7.4 is the preferred medium for dispersing NPs for most biological experiments. It is therefore realistic to measure the physical stability of either GAL-FNPs or FNPs aqueous PBS dispersions by monitoring mean size and width of distribution as a function of incubation time until 24 h. Results, reported in Fig. 3, showed that for both samples no significant changes in the initial mean size and width of distribution were observed after 7 h of incubation, indicating their high stability. However, after 24 h of incubation, this increase became significant for both GAL-FNPs and FNPs ( $p < 0.05$ ), suggesting that these nanoparticle dispersions can be used for biological analyses within 24 h after dispersion. On the contrary,  $\zeta$  potential values do not significantly change until 24 h of incubation.

### 3.5. In vitro experiments

The toxicity of galactosylated and/or pegylated FNPs was investigated upon incubation with human hepatoma cells (HepG2) or cervical cancer cells (HeLa) at different concentrations (0.5 mg/ml–0.1 mg/ml) for 24, 48 and 72 h.

HepG2 cells have been widely used for evaluating the interaction between galactose-mediated targeted systems and cells since they are known to express ASGPR on membrane surface [6,32]; on the contrary, HeLa cells, that don't express the receptor, were chosen as negative control. Results, in terms of cell viability after incubation in the presence of GAL-FNPs or FNPs, are reported in Fig. 6a (for HepG2) and in Fig. 6b (for HeLa).

As shown, the cytotoxicity was negligible at all tested concentrations and incubation times; on the contrary, at lower concentrations the particles with galactose seem to give a slight proliferative stimuli to HepG2; the same effect to HeLa cells was due to all nanoparticle samples during the first 24 h.

Finally, thanks to the fluorescence given by covalently-linked RhB it was evaluated, by confocal analysis, whether the uptake of

GAL-FNPs by HepG2 cells could be increased by the contributor of the ASGPR. In particular, HepG2 and HeLa cells were treated with GAL-FNPs (0.25 mg/ml) for 1, 3, or 5 h at 37 °C. After incubation, the cells were washed to remove any remaining particles and stained with phalloidin and DAPI to identify cellular compartment. Confocal images clearly showed GAL-FNPs inside HepG2 cells already 1 h after incubation (Fig. 7a), the amount of observed cytoplasmic particles reaches its peak after 3 h (Fig. 7b) with a reduction after 5 (Fig. 7c). On the contrary, at the same time points, no particles were found inside HeLa cells (Fig. 8).

To confirm that the GAL-FNPs uptake was resulted from a specific interaction between galactose and ASGPR, FNPs were used as negative controls. As shown in Fig. 9, no staining could be observed in HepG2 cells incubated with FNPs for 1, 3 and 5 h thus confirming the contribution and specificity of the ASGPR for the internalization of GAL-FNPs. This study clearly demonstrates that uptake of GAL-FNPs into hepatic cells occurs through the ASGPR via receptor-mediated endocytosis, according with results obtained by other authors [33–38].

## 4. Conclusions

In this work, the synthesis of a galactosylated copolymer bearing rhodamine B (RhB) moieties and its use for the preparation of polymeric fluorescent nanoparticles for potential in vitro and in vivo imaging applications are described. To do this, a sequence of functionalization reactions were performed on  $\alpha,\beta$ -poly(*N*-2-hydroxyethyl)-D,L-aspartamide (PHEA). In particular, a fluorescent derivative of PHEA was obtained by chemical reaction of PHEA with RhB. Then, a galactosylated derivative of polyethylene glycol, the O-(2-aminoethyl)-O'-galactosyl polyethylene glycol (GAL-PEG-NH<sub>2</sub>) was obtained by a reductive amination of lactose with primary amine function of poly(ethylene glycol)bis(amine) (H<sub>2</sub>N-PEG-NH<sub>2</sub>). Then, the fluorescent galactosylated polylactide-polyaminoacid conjugate was obtained by chemical reaction of PHEA-RhB with

poly(lactic acid) (PLA), and subsequent reaction with GAL-PEG-NH<sub>2</sub>, obtaining PHEA-RhB-PLA-PEG-GAL copolymer [11].

Starting from this copolymer, liver-targeted fluorescent nanoparticles (GAL-FNPs) were successfully prepared by high pressure homogenization (HPH)-solvent evaporation method. Obtained fluorescent nanoparticles have nanoscaled size, slightly negative zeta potential and spherical shape as showed by TEM images. Chemical and enzymatic stability of the ester linkage between fluorescent dye and copolymer was demonstrated until 4 days of incubation.

Finally, thanks to the fluorescence given by covalently-linked RhB it was demonstrated, by confocal microscopy studies, that FNPs bearing GAL moieties are endocytosed by HepG2 cells that are positive for the asialoglycoprotein receptor (ASGPR), while no internalization of particles was observed in HeLa cells that are negative for the same receptor, demonstrating the contributor of ASGPR to the internalization process.

## Acknowledgments

The authors thank MIUR for PRIN 20109PLMH2 and for FIRB RBFRI2NSCF, and University of Palermo for funding.

TEM were provided by Centro Grandi Apparecchiature – UniNetLab – Università di Palermo funded by P.O.R. Sicilia 2000–2006, Misura 3.15 Quota Regionale.

## References

- [1] A. Vollrath, S. Schubert, U.S. Schubert, J. Mater. Chem. 1 (2013) 1994.
- [2] C.-K. Huang, C.-L. Lo, H.-H. Chen, G.-H. Hsiue, Adv. Funct. Mater. 17 (2007) 2291.
- [3] T. Krasia-Christoforou, T.K. Georgiou, J. Mater. Chem. 1 (2013) 3002.
- [4] J. Mérian, J. Gravier, F. Navarro, I. Texier, Molecules 17 (2012) 5564.
- [5] C.-H. Lai, C.-Y. Lin, H.-T. Wu, H.-S. Chan, Y.-J. Chuang, C.-T. Chen, C.-C. Lin, Adv. Funct. Mater. 20 (2010) 3948.
- [6] E.F. Craparo, D. Triolo, G. Pitarresi, G. Giammona, G. Cavallaro, Biomacromolecules 4 (2013) 1838.
- [7] E.F. Craparo, M.C. Ognibene, M.P. Casaletto, G. Pitarresi, G. Teresi, G. Giammona, Nanotechnology 19 (2008) 485603.
- [8] E.F. Craparo, G. Teresi, M.L. Bondi, M. Licciardi, G. Cavallaro, Int. J. Pharm. 406 (2011) 135.
- [9] M. Licciardi, M. Di Stefano, E.F. Craparo, G. Amato, G. Fontana, G. Cavallaro, G. Giammona, Int. J. Pharm. 433 (2012) 16.
- [10] E.F. Craparo, C. Sardo, R. Serio, M.G. Zizzo, M.L. Bondi, G. Giammona, G. Cavallaro, Int. J. Pharm. 466 (2014) 172.
- [11] E.F. Craparo, G. Teresi, M.C. Ognibene, M.P. Casaletto, M.L. Bondi, G. Cavallaro, J. Nanopart. Res. 12 (2010) 2629.
- [12] G. Giammona, B. Carlisi, S. Palazzo, J. Polym. Sci. Polym. Chem. Ed. 25 (1987) 2813.
- [13] E.F. Craparo, G. Teresi, M. Licciardi, M.L. Bondi, G. Cavallaro, J. Biomed. Nanotechnol. 9 (2013) 1107.
- [14] T. Etrych, M. Jelinkova, B. Rihova, K. Ulbrich, J. Control. Release 73 (2001) 89.
- [15] A. Laurentin, C.A. Edwards, Anal. Chem. 315 (2003) 143.
- [16] W.-J. Lin, M.H. Chen, Carbohydr. Polym. 67 (2007) 474.
- [17] M. Vertzoni, J. Dressman, J. Butler, J. Hempenstall, C. Reppas, Eur. J. Pharm. Biopharm. 60 (2005) 413.
- [18] E. Galia, E. Nicolaides, D. Horter, R. Lobenberg, C. Reppas, J.B. Dressman, Pharm. Res. 15 (1998) 698.
- [19] H.-S. Chen, Forensic Sci. J. 6 (2007) 21.
- [20] I. Reho, V. Vilímov, P. Jendelov, V. Kubicek, D. Jirak, V. Herynek, M. Kapcalova, J. Kotek, J. Cerny, P. Hermann, I. Luke, J. Med. Chem. 54 (2011) 5185.
- [21] P. Liu, L. Qin, Q. Wang, Y. Sun, M. Zhu, M. Shen, Y. Duan, Biomaterials 33 (2012) 6739.
- [22] S. Papa, F. Rossi, R. Ferrari, A. Mariani, M. De Paola, I. Caron, F. Fiordaliso, C. Bisighini, E. Sammali, C. Colombo, M. Gobbi, M. Canovi, J. Lucchetti, M. Peviani, M. Morbidelli, G. Forloni, G. Perale, D. Moscatelli, P. Veglianesi, ACS Nano 7 (2013) 9881.
- [23] T. Nguyen, M.B. Francis, Org. Lett. 5 (2003) 3245.
- [24] M. Beija, C.A.M. Afonso, J.M.G. Martinho, Chem. Soc. Rev. 38 (2009) 2410.
- [25] E. Birtalan, B. Rudat, D.K. Komel, D. Fritz, S.B.L. Vollrath, U. Schepers, S. Brase, Pept. Sci. 96 (2011) 694.
- [26] E.F. Craparo, G. Cavallaro, M.L. Bondi, D. Mandracchia, G. Giammona, Biomacromolecules 7 (2006) 3083.
- [27] E.F. Craparo, B. Porsio, N. Mauro, G. Giammona, G. Cavallaro, Macromol. Rapid Commun. (2015), <http://dx.doi.org/10.1002/marc.201500154>.
- [28] Y.B. Patil, U.S. Toti, A. Khadair, L. Ma, J. Panyamet, Biomaterials 30 (2009) 859.
- [29] E.F. Craparo, B. Porsio, M.L. Bondi, G. Giammona, G. Cavallaro, Polym. Degrad. Stabil. 119 (2015) 56.
- [30] M.F. Francis, M. Cristea, Y. Yang, F.M. Winnik, Pharm. Res. 22 (2005) 209.
- [31] E. Roger, F. Lagarce, E. Garcion, J.P. Benoit, Nanomedicine 5 (2010) 287.
- [32] L. Li, H. Wang, Z.Y. Ong, K. Xu, P.L.R. Ee, S. Zheng, J.L. Hedrick, Y.-Y. Yang, Nano Today 5 (2010) 296.
- [33] Y.-C. Wang, X.-Q. Liu, T.-M. Sun, M.-H. Xiong, J. Wang, J. Control. Release 128 (2008) 32.
- [34] A. Suo, J. Qian, Y. Yao, W. Zhang, Int. J. Nanomedicine 5 (2010) 1029.
- [35] F. Suriano, R. Pratt, J.P.K. Tan, N. Wiradharma, A. Nelson, Y.-Y. Yang, P. Dubois, J.L. Hedrick, Biomaterials 31 (2010) 2637.
- [36] D.-Q. Wu, Z.-Y. Li, C. Li, J.-J. Fan, B. Lu, C. Chang, S.-X. Cheng, X.-Z. Zhang, R.-X. Zhuo, Pharm. Res. 27 (2010) 187.
- [37] C. Duan, J. Gao, D. Zhang, L. Jia, Y. Liu, D. Zheng, G. Liu, X. Tian, F. Wang, Q. Zhang, Biomacromolecules 12 (2011) 4335.
- [38] R. Yang, F. Meng, S. Ma, F. Huang, H. Liu, Z. Zhong, Biomacromolecules 12 (2011) 3047.